Angewandte Chemie

GDCh

Eine Zeitschrift der Gesellschaft Deutscher Chemiker

www.angewandte.de

Akzeptierter Artikel

Dieser Beitrag wurde nach Begutachtung und Überarbeitung sofort als "akzeptierter Artikel" (Accepted Article; AA) publiziert. Die deutsche Übersetzung wird gemeinsam mit der endgültigen englischen Fassung erscheinen. Die endgültige englische Fassung (Version of Record) wird ehestmöglich nach dem Redigieren und einem Korrekturgang als Early-View-Beitrag erscheinen und kann sich naturgemäß von der AA-Fassung unterscheiden. Leser sollten daher die endgültige Fassung, sobald sie veröffentlicht ist, verwenden. Für die AA-Fassung trägt der Autor die alleinige Verantwortung.

WILEY · VCH

RESEARCH ARTICLE

Oxidative Electrocyclization Assembles 2,2-Dimethyl-2*H*-pyran in Fungal Indole Alkaloids

Chengjie Zhang [+], Jingxuan Zhou [+], Wei Wang [+], Mingyu Liu [+], Yuanning Li, Xiang Sheng, [*] Lei Du, [*] and Shengying Li [*]

[†] C. Zhang, J. Zhou, M. Liu, Y. Li, S. Li, L. Du

State Key Laboratory of Microbial Technology, Shandong University, Qingdao, Shandong, 266237, China

S. Li

Laboratory for Marine Biology and Biotechnology, Qingdao Marine Science and Technology Center, Qingdao, Shandong, 266237, China

W. Wang, X. Sheng

State Key Laboratory of Engineering Biology for Low-Carbon Manufacturing, Tianjin Institute of Industrial Biotechnology, Chinese Academy of Sciences, Tianjin, 300308, China

National Center of Technology Innovation for Synthetic Biology, Tianjin, 300308, China

Y. Li

Institute of Marine Science and Technology, Shandong University, Qingdao, Shandong, 266237, China

[*] Email: lishengying@sdu.edu.cn (S.L.)

lei.du@sdu.edu.cn (L.D.)

shengx@tib.cas.cn (X.S.)

[+] These authors contributed equally to this work.

Supporting information for this article is given via a link at the end of the document

Abstract: Pericyclic reactions, such as cycloaddition and electrocyclization, are among the most useful approaches for constructing complex natural products with diverse biological activities. While enzymatic pericyclic reactions have been increasingly reported in recent years, there are only few examples of enzyme-mediated electrocyclization reactions. The 2,2-dimethyl-2*H*-pyran (DMP) ring plays a significant role in constituting many bioactive fungal and plant natural products. In this study, we characterize the *vsc* biosynthetic gene cluster of the DMP-containing natural product versicamide A (**1**) in *Aspergillus versicolor* DL0022. The biosynthetic route for DMP formation and biochemical functions of the involved enzymes are fully elucidated. Specifically, we reveal that the berberine bridge-like oxidoreductase VscB mediates a crucial oxidative process, followed by an electrocyclization to form a C−O bridge bond, thereby affording the key DMP ring. Structural simulation, molecular modeling, mutational analysis, and quantum chemical calculations elucidate the oxidative electrocyclization mechanism. The FAD cofactor of VscB/NotD' facilitates hydride abstraction at the C25 position of the substrate, while the key amino acid residue E529 acts as a general base to deprotonate the C6 hydroxyl group.

Introduction

Pericyclic reactions, represented by electrocyclization and cycloaddition (*e.g.*, Diels-Alder reaction) (Fig. 1A), are among the most useful chemical synthetic approaches to constructing various cyclic structures. These reactions are also widely adopted by microorganisms and plants to biosynthesize complex natural products with diverse biological activities[1-4]. Despite the extensive applications of pericyclic reactions in chemical synthesis, enzymatic pericyclic reactions in nature are relatively rare. Thus, the studies on biosynthetic pericyclic reactions are of great interest[5-7]. Over the past two decades, the majority of characterized enzymatic pericyclic reactions have fallen into cycloaddition[8-16]. By contrast, there are only few reports on enzymes that mediate electrocyclization[17-19]. Notably, two eukaryotic enzymes have been shown to control the stereochemical outcome of the electrocyclization reactions in the transformation of conjugated octaenes and nonaenes[17], while two prokaryotic enzymes, derived from *Streptomyces*, participate in benzene ring biosynthesis via electrocyclization[18, 19].

The 2,2-dimethyl-2*H*-pyran (DMP) ring, as a unique structural moiety, plays a significant role in constituting many biologically active fungal and plant natural products, such as indole alkaloids[20-22] from various *Aspergillus* and *Penicillium* species, acridone alkaloids[23, 24] from *Medicosma*, and precocenes[25, 26] from the herb *Ageratum* (Fig. 1B). Although chemical synthesis of the DMP ring has been achieved through thermally driven all-pericyclic reactions[27], there is a paucity of research on the enzymatic assembly of the DMP ring during biosynthesis of natural products. We and our collaborators previously proposed the biogenesis of the DMP ring in the biosynthetic pathways of some fungal indole alkaloids[28-30], such as notoamides and paraherquamides (Fig. S1). However, experimental evidence is unavailable, and the biosynthetic process of the DMP ring formation remains unclear.

In this study, we identified the biosynthetic gene cluster (BGC) of the DMP-containing natural product versicamide A (**1**) in *Aspergillus versicolor* DL0022 (*Av22*). The biosynthetic process and enzymes responsible for DMP formation were fully characterized. In particular, the berberine bridge-like enzyme (BBE) VscB/NotD' was revealed to mediate the oxidative electrocyclization to afford the key C−O bridge bond in the DMP

RESEARCH ARTICLE

ring of the intermediate notoamide E (**2**). The catalytic mechanism was elucidated through structural simulation, molecular modeling, mutational analysis, and quantum chemical calculations. Finally, phylogenetic analysis of VscB/NotD' and their homologues indicates their wide distribution in the fungal kingdom and novel functional classification in natural product biosynthesis.
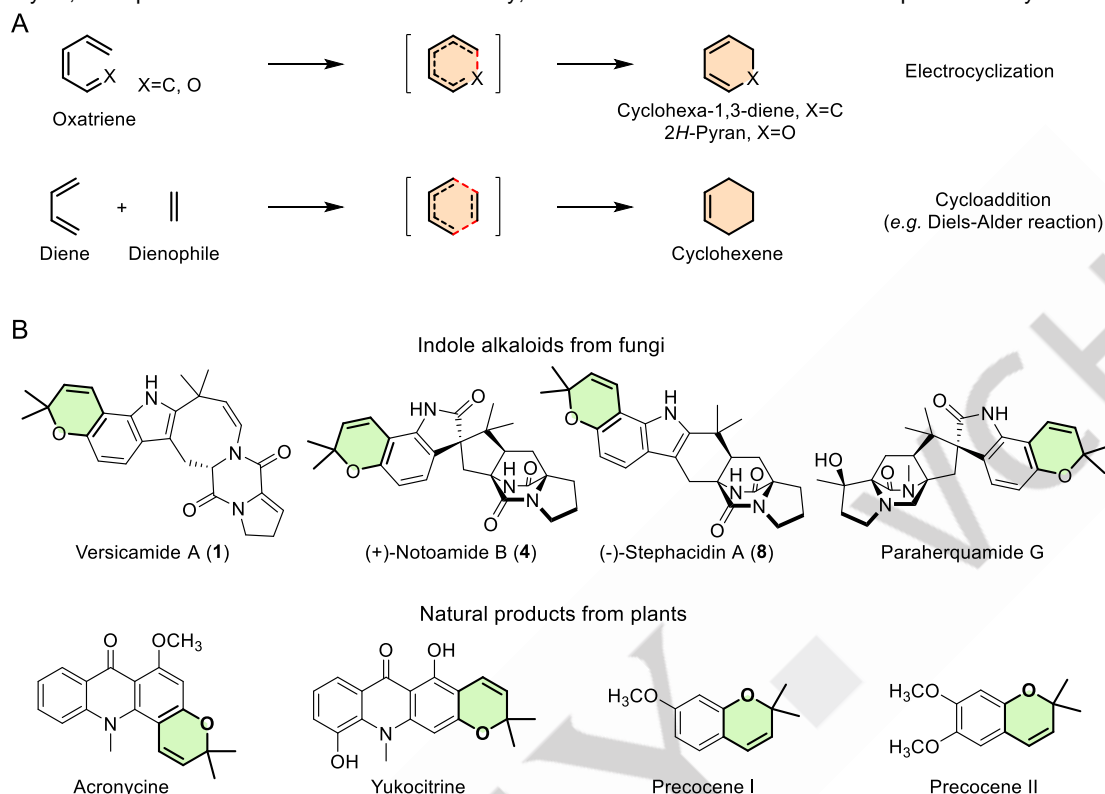

Figure 1. Two pericyclic reactions and 2,2-dimethyl-2*H*-pyran (DMP)-containing natural products. (A) Two canonical pericyclic reactions: electrocyclization and Diels-Alder cycloaddition. (B) Representative natural products featuring the DMP moiety (as highlighted in light green).

Results and Discussion

Identification of the versicamide A biosynthetic gene cluster

This laboratory has continuous interests in the biosynthesis of fungal indole alkaloids[29, 31-33]. Considering that *Aspergillus* species are potential fungal producers of these indole alkaloids, we isolated and collected a series of *Aspergillus* strains over the past decade. To discover potential fungal indole alkaloids, these *Aspergillus* strains were cultured in several different fungal-specific media for production of secondary metabolites. Through comprehensive analyses including high-performance liquid chromatography (HPLC), chromatographic purification, high-resolution mass spectrometry (HRMS), and nuclear magnetic resonance (NMR), a previously reported indole alkaloid **1**[34] which contains a DMP ring, was identified from an *A. versicolor* strain *Av22* (Figs. 1B and S11-S13). Structurally, **1** possesses a DMP ring, making it a good candidate for the biosynthetic studies on enzyme functions and catalytic mechanisms.

A significant portion of fungal indole alkaloids contain a DMP moiety, such as stephacidins and notoamides (Fig. 1B), which are derivatives of the cyclic dipeptide brevianamide F (**3**), a product of nonribosomal peptide synthetase (NRPS). Given the structural similarity of these indole alkaloids with compound **1**, we employed the known brevianamide F synthetase NotE[35] involved in notoamide biosynthesis as a sequence probe to perform protein BLAST searching in the *Av22* genome (Table S3), aiming to locate the BGC of versicamides. As a result, an NRPS gene with 59% amino acid sequence identity to NotE was revealed. By BGC analysis with antiSMASH[36] and further comparison of adjacent genes with the notoamide biosynthetic genes[35], we found a putative ~20 kb BGC (named "*vsc*") composed of seven genes (*vscA-E*, Fig. 2). Functional annotation and domain analysis showed that the encoded enzymes include one NRPS (VscA), one oxidoreductase (VscB), two prenyltransferases (VscC and VscE), two cytochrome P450 monooxygenases (VscD and VscF), and one Fe(II)/*α*-oxoglutarate-dependent oxygenase VscG (Table S4). Compound **1** was deduced to be a derivative of **3** with multiple modifications. Based on the predicted functions of the enzymes encoded by *vsc* (Fig. 2), we hypothesized that **1** should be the product of this BGC. To validate the hypothesis, the whole gene cluster (*vscA-G*) was heterologously expressed in *Aspergillus oryzae* M-2-3 (*Ao*)[37]. As expected, HPLC analytic results showed that the recombinant
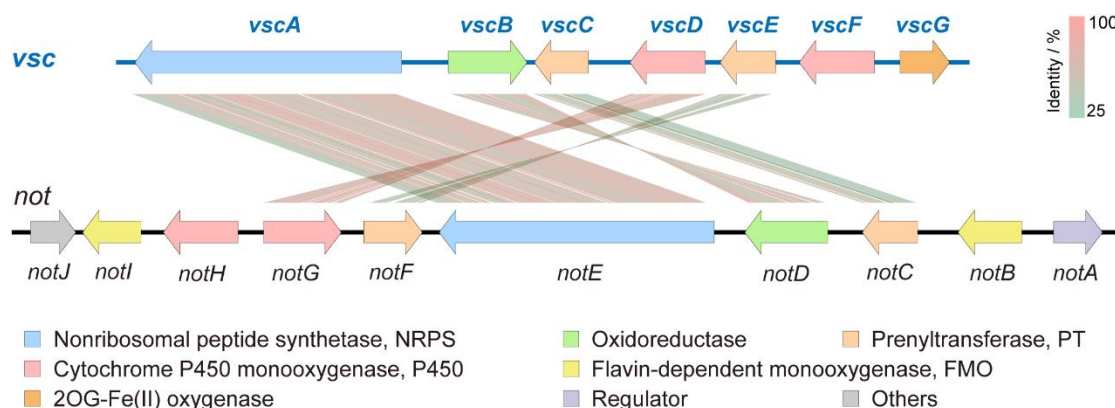
RESEARCH ARTICLE

Figure 2. Comparative analysis of the biosynthetic gene clusters *vsc* (for versicamide A) and *not* (for notoamides).

strain *Ao::vscABCDEFG* indeed produced **1** as the native producer strain *Av22* (Fig. 3A traces i and ii), demonstrating that the *vsc* cluster is responsible for biosynthesis of **1**.

Functional analysis of biosynthetic genes

The structure of **1** makes it a good candidate for understanding the biosynthetic mechanism of DMP. Since the structurally similar compound notoamide B (**4**) also contains a DMP substructure, we comparatively analyzed both BGCs (*vsc* and *not*) and found five homologous genes, namely, *vscA–E* and *notC–G* (Fig. 2). Thus, it is reasonable to infer that the biosynthetic genes responsible for DMP ring formation are likely among the five genes. To verify this inference, we heterologously co-expressed *vscA-E* in *Ao*. HPLC analysis of the metabolites of *Ao::vscABCDE* showed four new peaks with retention times of 11.6, 13.8, 17.0 and 20.1 min (Fig. 3B trace ii). Upon structural determination by HRMS (Fig. S11) and NMR (Figs. S14-S21) analyses, these four products were identified to be **3**, 6-hydroxydeoxybrevianamide E (**5**), deoxybrevianamide E (**6**) and **2**. Consistent with our hypothesis, **2** contains the DMP ring.

Subsequently, we sought to characterize the biochemical functions of the five biosynthetic enzymes (VscA–E) in order to understand how the DMP ring is assembled. The bimodular NRPS encoded by *vscA* with the A-T-C-A-T-C domain organization is presumed to catalyze the formation of the starting cyclodipeptide precursor **3**, which is a condensation product of L-tryptophan and L-proline. Its homologs BvnA (47%/63%, protein sequence identity/similarity) and NotE (59%/72%) were previously characterized to be responsible for generating **3** in the biosynthesis of brevianamides and notoamides, respectively[31, 35]. Expectedly, compared with the control wild-type *Ao*, the *Ao::vscA* strain with heterologously expressed VscA produced **3** (Fig. 3B trace iii).

Bioinformatics analysis indicates that VscE is a prenyltransferase showing protein sequence identity/similarity of 43%/58% and 42%/57% with its homologs BvnC[31] and NotF[35], respectively. The putative function of VscE is to catalyze a prenylation reaction of **3**. To confirm this, two strains *Ao::vscE* (for expression of VscE) and *Ao::vscAE* (for co-expression of VscA and VscE) were constructed. As expected, *in vivo* experiments showed that the prenylated product **6** was

generated by both *Ao::vscE* when fed with **3** (Fig. 3C trace ii) and *Ao::vscAE* (Fig. 3B trace iv). Of note, prenylation plays an important role in structural diversification of natural products[35].

Based on biosynthetic logic, the remaining three enzymes including cytochrome P450 enzyme VscD, prenyltransferase VscC, and oxidoreductase VscB were hypothesized to mediate DMP assembly. Thus, we constructed the three recombinant strains *Ao::vscD*, *Ao::vscC* and *Ao::vscB*. Precursor feeding experiments showed that only *Ao::vscD* was able to recognize **6** and generated a new peak with the retention time of 13.8 min (Fig. 3C trace iv and Fig. S2), which was determined to be the C6-hydroxylated product **5** by HRMS and NMR analyses (Figs. S18-S19). Consistently, the strain *Ao::vscAED* with co-expression of VscA, VscE and VscD also generated **5**. These *in vivo* experiments clearly demonstrated that VscD catalyzes the C6-hydroxylation of **6**, giving rise to **5**.

To characterize the following biosynthetic steps, *Ao::vscC* and *Ao::vscB* were individually fed with **5**. Surprisingly, HPLC results showed that no obvious product peaks were detected for both strains (Fig. 3C trace vi and Fig. S3). Nonetheless, mass spectrometric analysis showed that *Ao::vscC* produced a new product **7** in small amount with *m/z* value of 436 ([M+H]⁺) (Fig. S4A), suggesting addition of an isopentenyl unit to **5**. We reasoned that the low conversion rate might be due to the difficulty of **5** in passing through the fungal cell membrane since a similar phenomenon was previously observed in another study of fungal natural product (mycophenolic acid) biosynthesis[38]. To validate this hypothesis, we conducted additional experiments by incubating **5** with cell lysates of the *Ao::vscC* strain. LC-MS results showed a markedly higher product yield in the cell lysate reaction compared to the feeding experiment (Fig. S4), consolidating that **5** should have poor cell membrane permeability. To address this issue, a recombinant strain *Ao::vscDC* was constructed to co-express VscD and VscC, where the expression of VscD should intracellularly generate **5** from **6**. As expected, feeding of **6** to *Ao::vscDC* resulted in the production of **5** (the product of VscD) and **7** (the product of VscC) (Fig. 3C trace viii), clearly indicating that the biosynthetic step following the VscD-mediated C6-hydroxylation is catalyzed by prenyltransferase VscC. Supporting this, strain *Ao::vscAEDC* also produced the same product **7** (Fig. 3B trace vi). Compound **7** was purified and structurally elucidated to be notoamide S, a

known intermediate in notoamides biosynthesis (Figs. S11, S22-S23). All these results indicate that VscC is a notoamide S synthase by catalyzing the C7-prenylation of **5**. Although the two
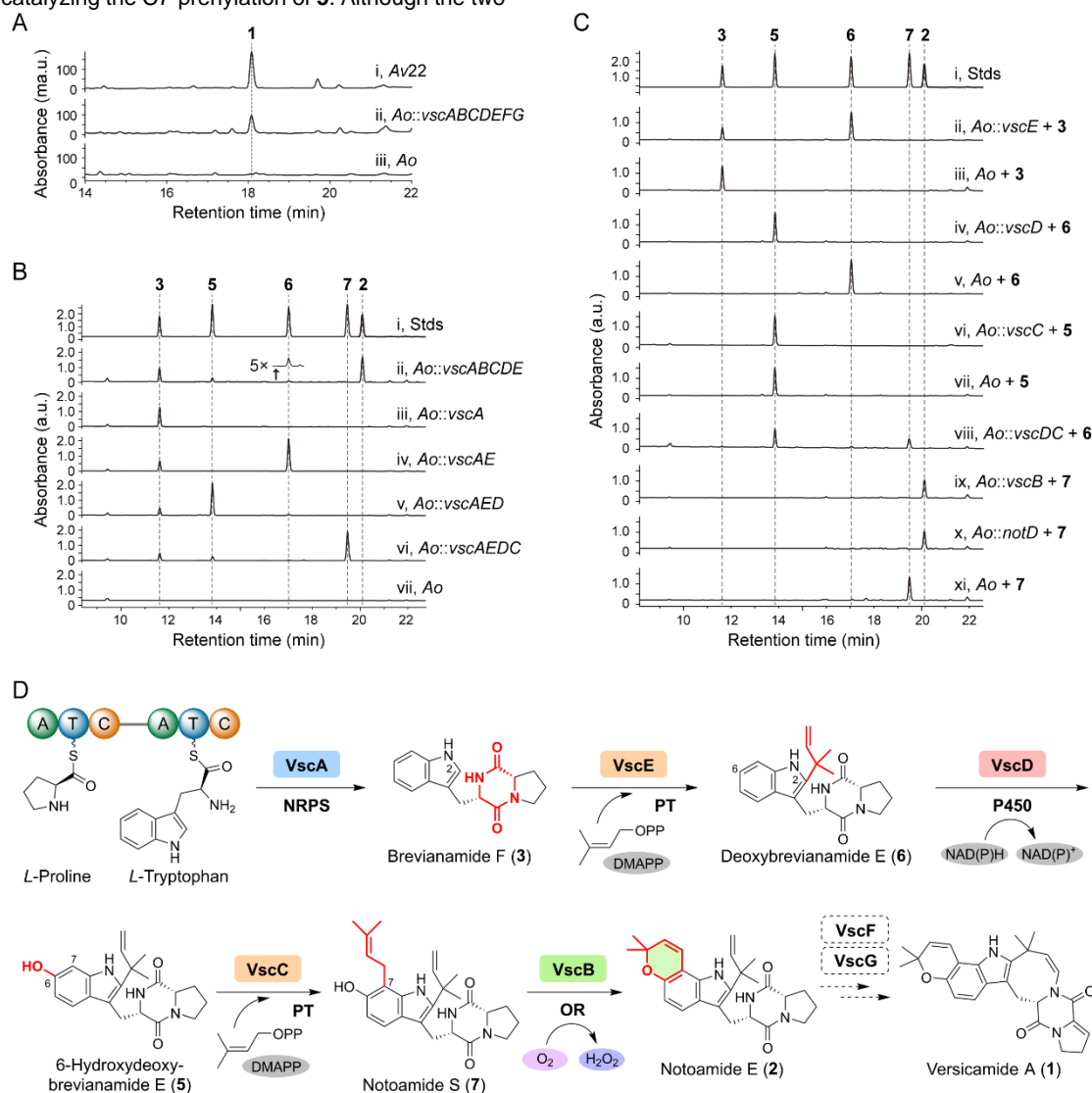

Figure 3. Functional characterization of VscA–E with the focus on 2,2-dimethyl-2*H*-pyran (DMP) biosynthesis. (A) HPLC analysis of the metabolites of *A. versicolor* DL0022 (*Av22*) and *Ao::vscABCDEFG* (*A. oryzae* M-2-3 (*Ao*) with *vscA–G* co-expressed). (B) HPLC analysis of the metabolites of recombinant *Ao* strains with heterologous expression of different combinations of *vscA–E* genes. (C) HPLC analysis of the precursor feeding experiments. (D) The characterized biosynthetic pathway leading to the DMP formation in notoamide E. The DMP moiety was highlighted in light green. Key bond formations occurring at each reaction step are marked in red.

prenyltransferases (VscE and VscC) in the same BGC share a certain degree of homology (28%/46%, protein sequence identity/similarity), they display distinct substrate specificity and regioselectivity.

In consideration of the result that *Ao::vscABCDE* produced **2** (Fig. 3B trace ii and Fig. S11, S20-S21) and the determined catalytic functions of VscA, VscC, VscD and VscE as described above, it is reasonable to deduce that the final oxidative cyclization step leading to the DMP ring should be mediated by the oxidoreductase VscB. As expected, when we fed **7** to *Ao::vscB*, this intermediate was entirely converted into **2** by this

strain (Fig. 3C trace ix), confirming the presumed functionality of VscB.

Taken together, the biosynthetic pathway for **2** comprises five enzymes: VscA, VscE, VscD, VscC, and VscB, which mediate the dipeptide condensation and cyclization, C2-prenylation, C6-hydroxylation, C7-prenylation, and oxidative cyclization, sequentially (Fig. 3D). Of note, the intermediate **6** produced by VscA and VscE, is a common precursor to many other diketopiperazine alkaloids, such as brevianamides, notoamides and stephacidins[30, 39]. Additionally, we propose that the remaining two enzymes encoded by the *vsc* gene cluster (the P450 monooxygenase VscF and the Fe(II)/2-oxoglutarate-

dependent oxygenase VscG) are likely involved in the post-modification of **2** to yield the final product **1** (Fig. 3D) , which will be confirmed by this laboratory in a due course.

Our functional analysis demonstrated that the oxidoreductase VscB is the key enzyme responsible for the DMP ring formation.

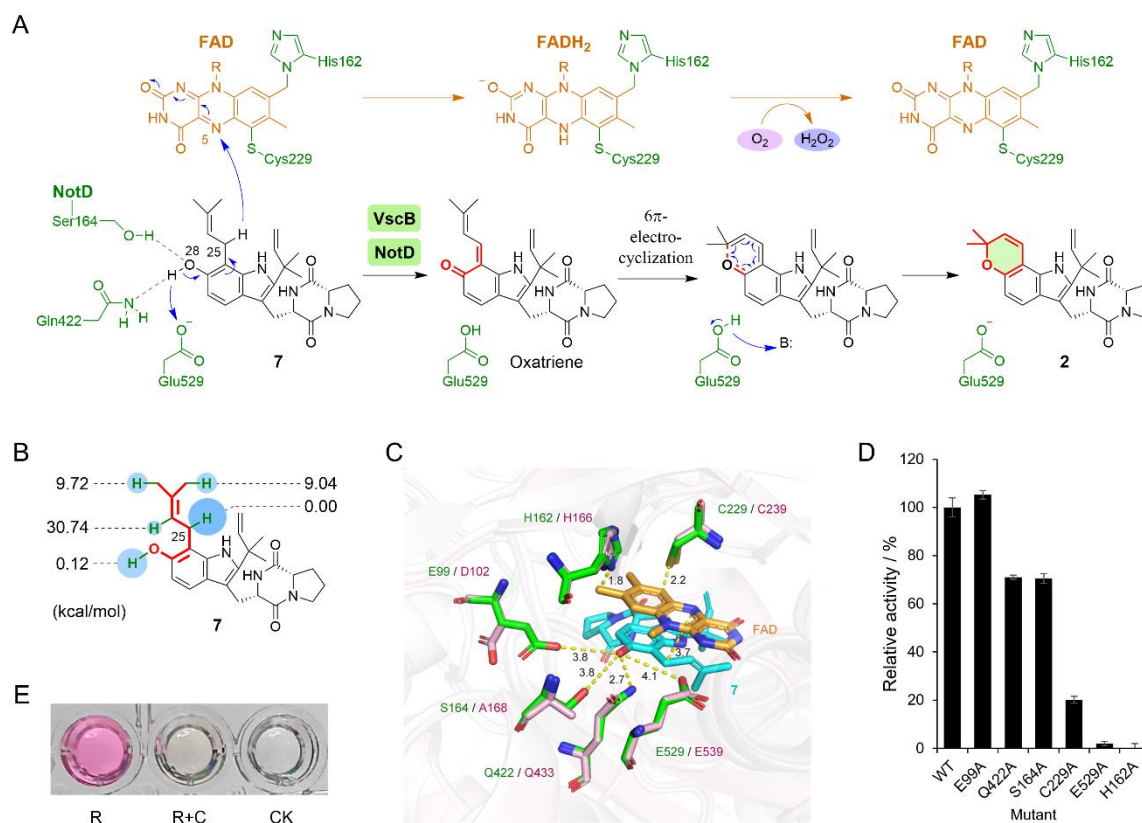## Probing the catalytic mechanism of the oxidoreductase VscB/NotD'

Figure 4. Elucidation of the catalytic mechanism of VscB/NotD'. (A) Proposed mechanism for VscB/NotD'-mediated oxidative electrocyclization. (B) Quantum chemical calculations of bond dissociation energies. The secondary C−H bond at the C25 position has the lowest bond dissociation energy. (C) The docked NotD'-**7** complex with the key residues shown, overlaid with VscB; NotD' and VscB residues are shown in green and pink, respectively. Distances are indicated in Å. (D) Site-directed mutagenesis results. Data are presented as mean ± standard deviations (n = 3 biologically independent samples). (E) H_2O_2 detection with Amplex Red reagent. R, NotD' *in vitro* reaction. R+C, the NotD' reaction with added catalase, which can catalyze the breakdown of hydrogen peroxide produced in the reaction. CK, control reaction with boiling-inactivated NotD'.

Conserved domain analysis showed that this enzyme possesses a flavin adenine dinucleotide (FAD) binding domain and a BBE domain[40] (Fig. S5). Based on the structure of its substrate **7** and chemical principles, we proposed a concerted mechanism involving oxidative electrocyclization (Fig. 4A). In this putative mechanism, FAD acts as a catalytic cofactor to facilitate hydride abstraction. Hypothetically, the N5 atom of FAD receives the hydride transferred from the C25 position of **7**. Supporting this hypothesis, quantum chemical calculations indicate that the secondary C−H bond at the C25 position has the lowest bond dissociation energy (Fig. 4B). Meanwhile, an ionizable residue may serve as a general base to abstract a proton from the O28 position of **7**. The simultaneous elimination of the hydride and proton generates an oxatriene intermediate, which then undergoes a 6π-electrocyclic ring closure to yield **2** containing the DMP substructure.

To further investigate the catalytic mechanism and identify the key amino acid residues of the oxidoreductase VscB *in vitro*, we initially attempted to express this protein in *Escherichia coli*. However, no active VscB protein was obtained from *E. coli* BL21(DE3), suggesting this eukaryotic enzyme could not be expressed in the prokaryotic host. Thus, we switched to use the eukaryotic host *Ao* for protein preparation. To increase success rate, we constructed the fungal expression vectors for VscB and its homolog NotD' (NCBI accession number L7WR40; exhibiting 57%/74% protein sequence identity/similarity to VscB) with an *N*- or *C*-terminal His$_6$-tag and individually transformed them into *Ao*. NotD' is an oxidoreductase with uncharacterized function from the notoamide biosynthetic pathway (Fig. S1). Based on their homology and our previous proposal for the biosynthetic pathway of notoamides[28-30], we speculated that NotD' might also catalyze the same reaction as VscB (Fig. S1). By heterologous expression and feeding experiments, we confirmed that NotD'

RESEARCH ARTICLE

was able to mediate the same conversion of **7** to **2**, as VscB does (Fig. 3C trace x). Following a liter-scale fermentation, Ni-NTA affinity chromatography was used for enrichment and purification of the His-tagged proteins. For VscB, no obvious target band could be detected in SDS-PAGE analysis. To our delight, we obtained enough NotD' protein from *Ao* and purified it to near homogeneity (Fig. S7). Protein mass spectrometric analysis verified that the purified enzyme matched the target protein NotD' (Table S6 and Fig. S8). Subsequent *in vitro* enzymatic assays

using the purified NotD' unequivocally validated its oxidative cyclization activity, converting **7** into **2** (Figs. 4D and S9).

To identify the catalytically relevant amino acid residues of NotD', we proceeded with crystallization screening on the purified protein, aiming to obtain the protein-substrate complex structure. However, our greatest efforts turned out to be unsuccessful. Thus, we alternatively performed structural simulation with AlphaFold2[41] and investigated the interactions of NotD' with **7** by molecular docking with AutoDock Vina[42].
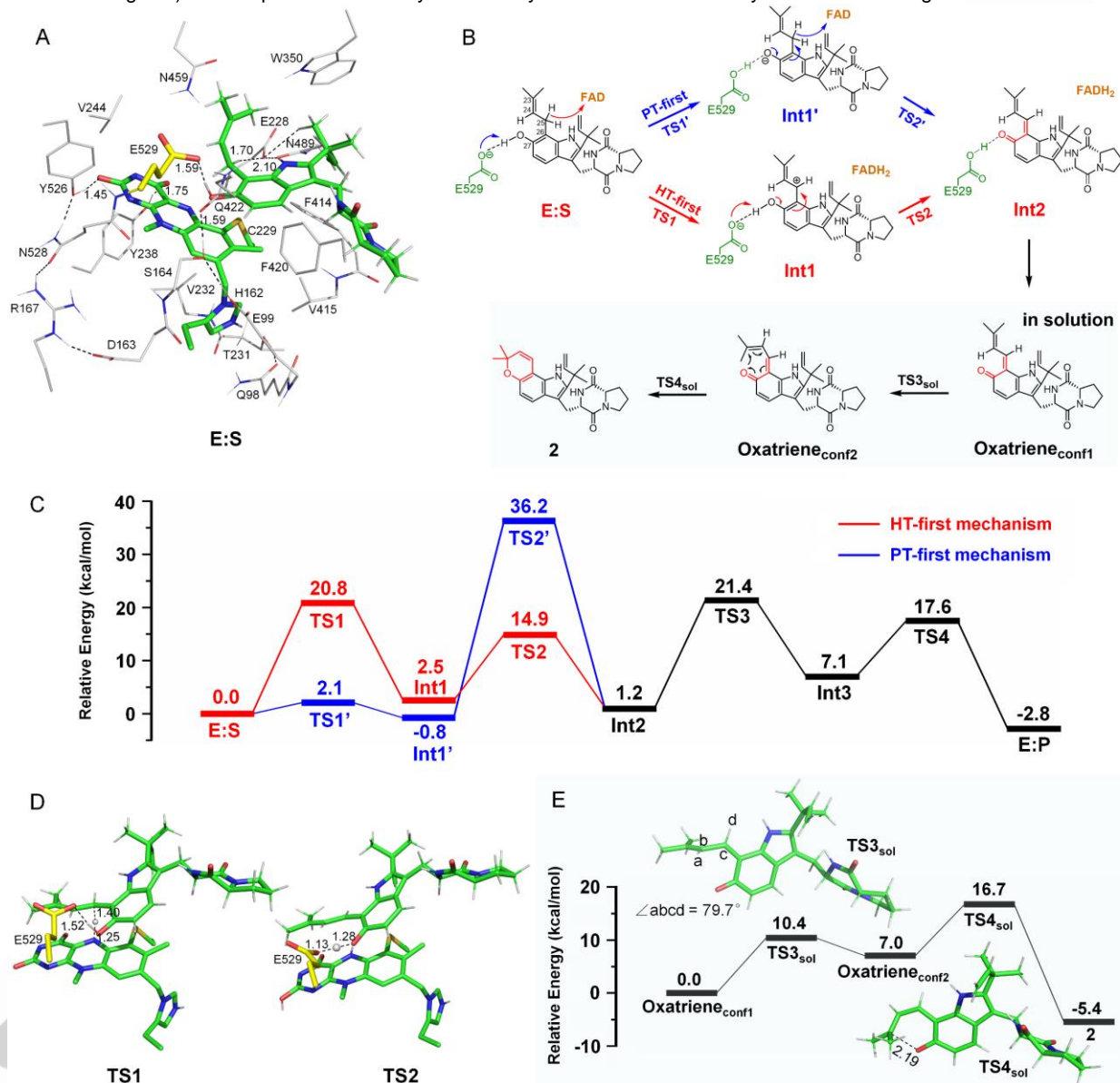

Figure 5. Results of quantum chemical calculations. (A) Optimized structure of E:S. (B) The hydrogen transfer (HT)-first and proton transfer (PT)-first mechanisms investigated in this study. (C) Calculated energy profiles for HT-first and PT-first mechanisms of NotD' with the reaction taking place in enzyme. The HT-mechanism has feasible energies, while the PT-first mechanism is calculated to be associated with a prohibitively high barrier. (D) Optimized structures of the transition states of HT and PT steps involved in the HT-first mechanism. Only a part of the model is shown in these two structures (see Fig. 5A for the full model). (E) Calculated energy profile for the conformational change and cyclization reaction taking place in solution, showing that these two steps have lower barriers than those in enzyme. For clarity, most of the nonpolar hydrogens are not displayed in the optimized structures. Selected distances are given in angstrom.

In the modeled enzyme-substrate-cofactor complex, the key amino acids (H162 and C229 in NotD', H166 and C239 in VscB) that bind to FAD were found to be conserved (Figs. 4C and S10).

Site-directed mutagenesis analysis showed that the mutant H162A completely lost the ability to catalyze the DMP ring formation, while the mutant C229A retained 20.2% activity

WILEY-VCH

RESEARCH ARTICLE

relative to the wild-type enzyme (Fig. 4D). These results indicate that these two residues are crucial for FAD binding and hence catalytic activity, consistent with other BBE-like proteins[43]. Based on the proposed catalytic mechanism (Fig. 4A) and molecular docking analysis (Fig. 4C), amino acid residues E99, S164, Q422 and E529 within 5 Å distance around the hydroxyl group of **7** are likely to act as the key residues for deprotonation. To test this hypothesis, we mutated each amino acid to alanine and evaluated the *in vitro* activities of the four mutants. Specifically, the mutant E99A demonstrated comparable activity to the wild type enzyme, suggesting that this residue might not participate in the catalytic process. The E529A mutation almost completely abolished the activity of NotD', while mutants S164A and Q422A showed 70.5% and 71.0% relative activities, respectively (Fig. 4D). These results suggested that E529 might be the key base for deprotonation of the hydroxyl group during the oxidative electrocyclization process. S164 and Q422 could play an auxiliary role via forming hydrogen bonds with the hydroxyl group of **7** to stabilize the substrate transition states during the catalytic process. This may explain why the activity of VscB was lower than that of NotD' in the feeding experiments (Fig. S6) since S164 of NotD' is replaced by an alanine (A168) in VscB. Additionally, molecular oxygen would re-oxidize the reduced FAD and produce hydrogen peroxide (H_2O_2) as a byproduct in the catalytic cycle, according to the known mechanism of BBE domain-containing oxidoreductases[43]. Supporting this, the production of H_2O_2 was detected in the *in vitro* NotD' reaction through a peroxidase-mediated colorimetric assay using the Amplex Red reagent[44] (Fig. 4E).

Quantum chemical calculations

To further investigate the detailed mechanism of the oxidative electrocyclization, quantum chemical calculations were conducted. To determine the most stable binding mode of the substrate, we optimized a number of structures with different conformations of substrate and active site residues for the enzyme-FAD-substrate complexes. The lowest-energy one (E:S) is shown in Figure 5A, while alternative structures are provided in Figure S24. Starting from the enzyme-substrate-cofactor complex (E:S in Fig. 5A), the reaction may initiate through either a hydride transfer (HT) from the substrate to FAD or a proton transfer (PT) from the substrate hydroxyl group to Glu529 (Fig. 5B, S25 and S26), referred to as the HT-first mechanism and PT-first mechanism, respectively. To evaluate

the energetic feasibility of these two pathways, we established their energy profiles (Fig. 5C).

For the HT-first mechanism, starting from E:S, the reaction initiates with the hydride transfer from the substrate C25 to FAD (Fig. 5B). At the corresponding transition state (TS1, Fig. 5D), the distance between the transferring hydrogen of the substrate and the N5 of the cofactor is shortened to 1.25 Å from 2.57 Å in E:S. The calculated barrier for this hydride transfer is 20.8 kcal/mol, leading to the formation of an arenium ion intermediate (Int1 in Fig. S27), which is 2.5 kcal/mol higher than that of E:S (Fig. 5C). Following this, Glu529 is protonated by the phenolic hydroxyl group of the substrate. This protonation step has a barrier of 12.4 kcal/mol relative to Int1; that is, 14.9 kcal/mol relative to that of E:S (Fig. 5C). The resulting intermediate (Int2) is 1.2 kcal/mol higher in energy than E:S. For the PT-first mechanism (Fig. 5B), the proton transfer is calculated to be associated with a low barrier of only 2.1 kcal/mol (Fig. 5C), but the barrier of hydride transfer is as high as 37.0 kcal/mol relative to Int1' (Int1' in Fig. S28). Therefore, the proton transfer from the substrate to Glu529 renders the hydride transfer from the substrate to FAD energetically infeasible. This can be evidenced by the difference in the key geometry parameters in E:S and Int1' (Fig. S29). Namely, the angle of C25-H-N5 is less linear in Int1' (127.7°) compared to that in E:S (155.7°), and the length of N5-H is longer in Int1' (3.05 Å) than that in E:S (2.67 Å). These results suggest that the reaction should proceed via the HT-first mechanism rather than the PT-first mechanism.

After Int2, the isobutenyl group requires a conformational change to facilitate the cyclization via a C-O bond formation (Fig. 5B). The calculations show that the conformational change in enzyme is associated with a barrier of 21.4 kcal/mol and the cyclization has a barrier of 17.6 kcal/mol, relative to E:S (Fig. 5C). Analysis of the transition state structures shows that the high barrier for the conformational change can be attributed to the steric hindrance between the isobutenyl group and active site residues (Fig. S30). Indeed, the calculated barrier for this conformational change in solution (10.4 kcal/mol, TS3$_{sol}$ in Fig. 5E) is much lower than that in enzyme (20.2 kcal/mol relative to Int2, TS3 in Fig. 5C). The barrier of the following cyclization step in solution (9.7 kcal/mol relative to Int3$_{sol}$, TS4$_{sol}$ in Fig. 5E) is similar to that in enzyme (10.5 kcal/mol relative to Int3, TS4 in Fig. 5C). The distance of the forming C-O bond at TS4$_{sol}$ is 2.19 Å. Taken together, these results suggest that the final cyclization step unlikely occurs within the enzyme pocket but instead prefers to occurring spontaneously after the intermediate Int2 being released to the solution.
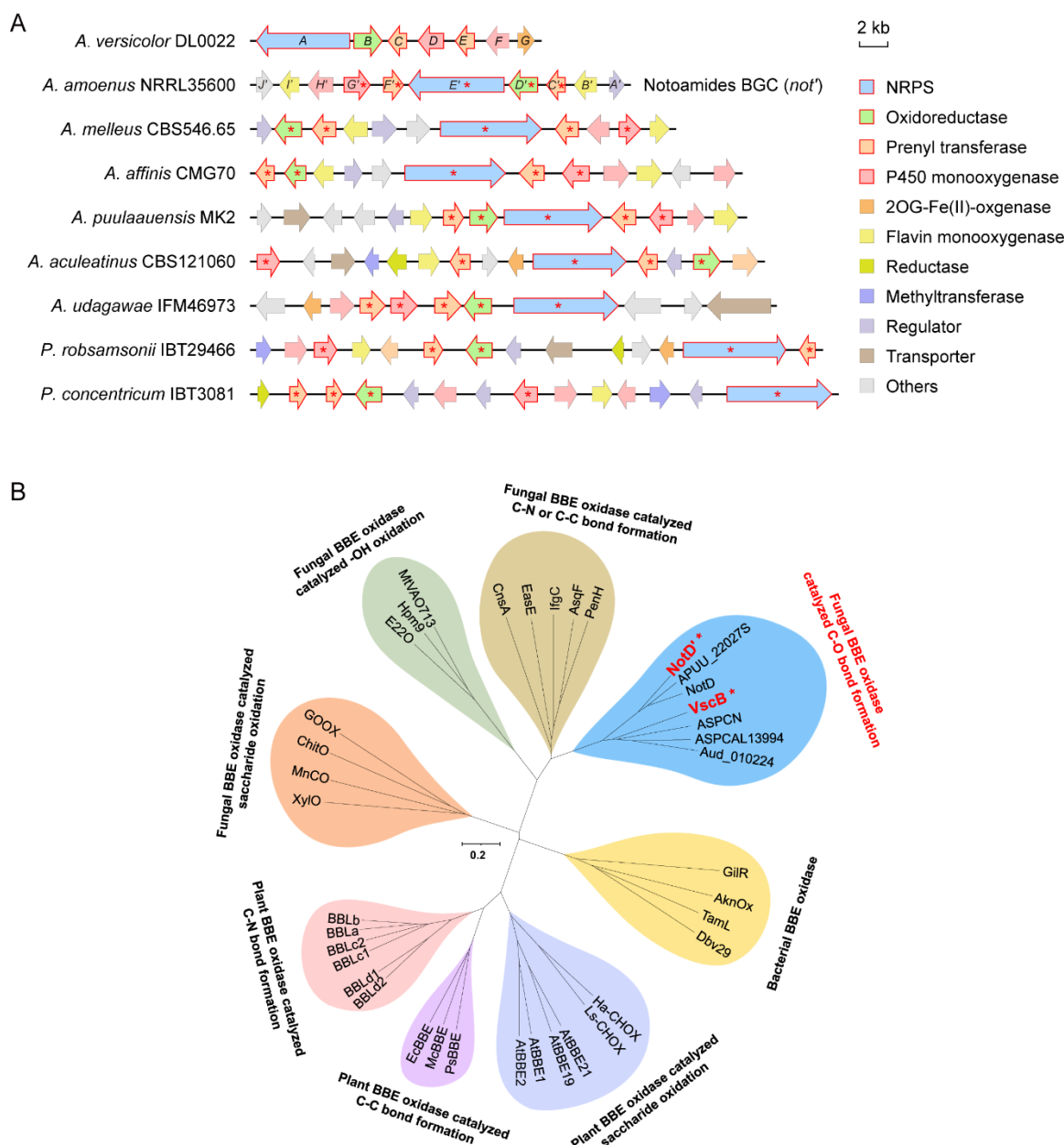
RESEARCH ARTICLE

Figure 6. Bioinformatics analysis of *vsc*-homologous biosynthetic gene clusters (BGCs) and enzymes. (A) Comparison of *vsc*-like BGCs from various fungal genomes. The *vsc*-homologs involved in the biosynthesis of notoamide E (**2**) are indicated by asterisks and outlined in red arrows. (B) Phylogenetic analysis of VscB/NotD' homologs as well as other BBE domain containing enzymes. VscB/NotD' (highlighted in red, asterisked) and their homologues form a distinct clade. Detailed information for the related proteins is provided in Table S5.

Evolutionary analysis

Bioinformatics analysis revealed that the *vsc*-like BGCs and VscB/NotD' homologs are widely distributed in many fungal genomes (Fig. 6A and Fig. S10). It is noteworthy that the majority of representative BBE enzyme-family oxidases have been characterized in plants, which mediate many pivotal oxidative cyclization reactions during benzylisoquinoline alkaloids biosynthesis[43]. BBE stereoselectively catalyzes the formation of the berberine bridge in (*S*)-scoulerine through phenolic coupling—a C−C bond-forming reaction critical for protoberberine alkaloid diversification. The functional divergence underscores the evolutionary plasticity of this type of flavin-

dependent oxidases in adapting to specialized metabolic pathways across different kingdoms. Comparatively, our characterization of the fungal BBE homolog reveals a functional shift towards prenylated diketopiperazine substrates. Given that these BGCs contain the five *vsc* homolog genes (*i.e.*, *vscAEDCB*) involved in the biosynthesis of compound **2** and variable post-modification genes, we speculate that **2** might be a common intermediate for biosynthesis of diverse indole alkaloids. Comparative phylogenetic analysis showed that VscB/NotD'-like enzymes form a clade distinct from other BBE enzymes of fungal, plant and bacterial origins (Fig. 6B), suggesting that VscB/NotD'-like enzymes may represent a new class of oxidoreductases

WILEY-VCH

RESEARCH ARTICLE

containing BBE domain. Unlike the previously characterized BBE enzymes that catalyze C−C or C−N bond formation, and hydroxyl dehydrogenation, *etc.*[43], VscB/NotD' mediates a rare oxidative electrocyclization resulting in the formation of a C−O bridge bond. The widespread distribution of VscB/NotD'-like enzymes in fungal genomes implies their significant role in post-modification of fungal natural products.

Conclusion

In this study, the BGC of natural product **1** from *Av22* was investigated by focusing on the biosynthetic mechanism for the DMP moiety. Through integrated *in vivo* and *in vitro* experiments, the biosynthetic pathway and biochemical reactions involved in the DMP formation were fully elucidated. The oxidative electrocyclization mechanism mediated by the intriguing oxidoreductase VscB/NotD' was elucidated by structural simulation, molecular docking, site-directed mutagenesis, and quantum chemical calculations. The clarification of the DMP ring closure resolves the long-standing mystery on the key step in the biosynthesis of fungal indole alkaloids with this unique substructure. Bioinformatics analysis presents new enzyme resources, especially considering the broad distribution of VscB/NotD'-like oxidoreductases, for building synthetic biology modules to generate more "unnatural" DMP-containing natural products with potential biological activities for practical applications.

Acknowledgements

Conflict of Interest

The authors declare no conflict of interest.

Data Availability Statement

The data that support the findings of this study are available in the supplementary material of this article.

[1] Y. Jiang, R. E. McNamee, P. J. Smith, A. Sozanschi, Z. Tong, E. A. Anderson, *Chem. Soc. Rev.* **2021**, 50, 58−71.

[2] R. Ardkhean, D. F. J. Caputo, S. M. Morrow, H. Shi, Y. Xiong, E. A. Anderson, *Chem. Soc. Rev.* **2016**, 45, 1557−1569.

[3] K. Takao, R. Munakata, K. Tadano, *Chem. Rev.* **2005**, 105, 4779−4807.

[4] M. Juhl, D. Tanner, *Chem. Soc. Rev.* **2009**, 38, 2983−2992.

[5] C. S. Jamieson, M. Ohashi, F. Liu, Y. Tang, K. N. Houk, *Nat. Prod. Rep.* **2019**, 36, 698−713.

[6] B.-S. Jeon, S.-A. Wang, M. W. Ruszczycky, H.-W. Liu, *Chem. Rev.* **2017**, 117, 5367−5388.

[7] A. Minami, H. Oikawa, *J. Antibiot.* **2016**, 69, 500−506.

[8] S. M. Ma, J. W. H. Li, J. W. Choi, H. Zhou, K. K. M. Lee, V. A. Moorthie, X. Xie, J. T. Kealey, N. A. Da Silva, J. C. Vederas, Y. Tang, *Science* **2009**, 326, 589−592.

[9] H. J. Kim, M. W. Ruszczycky, S.-H. Choi, Y.-N. Liu, H.-W. Liu, *Nature* **2011**, 473, 109−112.

[10] M. Ohashi, F. Liu, Y. Hai, M. Chen, M.-C. Tang, Z. Yang, M. Sato, K. Watanabe, K. N. Houk, Y. Tang, *Nature* **2017**, 549, 502−506.

[11] M. Ohashi, C. S. Jamieson, Y. Cai, D. Tan, D. Kanayama, M.-C. Tang, S. M. Anthony, J. V. Chari, J. S. Barber, E. Picazo, T. B. Kakule, S. Cao, N. K. Garg, J. Zhou, K. N. Houk, Y. Tang, *Nature* **2020**, 586, 64−69.

[12] Q. Dan, S. A. Newmister, K. R. Klas, A. E. Fraley, T. J. McAfoos, A. D. Somoza, J. D. Sunderhaus, Y. Ye, V. V. Shende, F. Yu, J. N. Sanders, W. C. Brown, L. Zhao, R. S. Paton, K. N. Houk, J. L. Smith, D. H. Sherman, R. M. Williams, *Nat. Chem.* **2019**, 11, 972−980.

[13] S. Li, A. N. Lowell, F. Yu, A. Raveh, S. A. Newmister, N. Bair, J. M. Schaub, R. M. Williams, D. H. Sherman, *J. Am. Chem. Soc.* **2015**, 137, 15366−15369.

[14] Z. Tian, P. Sun, Y. Yan, Z. Wu, Q. Zheng, S. Zhou, H. Zhang, F. Yu, X. Jia, D. Chen, A. Mandi, T. Kurtan, W. Liu, *Nat. Chem. Biol.* **2015**, 11, 259−265.

[15] W. J. Wever, J. W. Bogart, J. A. Baccile, A. N. Chan, F. C. Schroeder, A. A. Bowers, *J. Am. Chem. Soc.* **2015**, 137, 3494−3497.

[16] B. Zhang, K. B. Wang, W. Wang, X. Wang, F. Liu, J. Zhu, J. Shi, L. Y. Li, H. Han, K. Xu, H. Y. Qiao, X. Zhang, R. H. Jiao, K. N. Houk, Y. Liang, R. X. Tan, H. M. Ge, *Nature* **2019**, 568, 122−126.

[17] K. Niwa, M. Ohashi, K. Xie, C.-Y. Chiang, C. S. Jamieson, M. Sato, K. Watanabe, F. Liu, K. N. Houk, Y. Tang, *J. Am. Chem. Soc.* **2023**, 145, 13520-13525.

[18] J. Zhang, S. Yuzawa, W. L. Thong, T. Shinada, M. Nishiyama, T. Kuzuyama, *J. Am. Chem. Soc.* **2021**, 143, 2962-2969.

[19] J. Shi, Y. Shi, J. C. Li, W. Wei, Y. Chen, P. Cheng, C. L. Liu, H. Zhang, R. Wu, B. Zhang, R. H. Jiao, S. Yu, Y. Liang, R. X. Tan, H. M. Ge, *J. Am. Chem. Soc.* **2022**, 144, 7939-7948.

[20] H. Kato, T. Yoshida, T. Tokue, Y. Nojiri, H. Hirota, T. Ohta, R. M. Williams, S. Tsukamoto, *Angew. Chem. Int. Ed.* **2007**, 46, 2254–2256.

[21] S. E. Blanchflower, R. M. Banks, J. R. Everett, C. Reading, *J. Antibiot.* **1993**, 46, 1355–1363.

[22] X.-M. Hou, T.-M. Liang, Z.-Y. Guo, C.-Y. Wang, C.-L. Shao, *Chem. Commun.* **2019**, 55, 1104–1107.

[23] A. Chukaew, C. Ponglimanont, C. Karalai, S. Tewtrakul, *Phytochemistry* **2008**, 69, 2616–2620.

[24] Q. C. Nguyen, T. T. Nguyen, R. Yougnia, T. Gaslonde, H. Dufat, S. Michel, F. Tillequin, *Anti-Cancer Agents Med. Chem.* **2009**, 9, 804–815.

[25] R. A. Halpin, K. P. Vyas, S. F. Elnaggar, D. M. Jerina, *Chem. Biol. Interact.* **1984**, 48, 297–315.

[26] T. Furukawa, N. Sakamoto, M. Suzuki, M. Kimura, H. Nagasawa, S. Sakuda, *PLoS One* **2015**, 10, e0135031.

[27] D. Tejedor, A. Diaz-Diaz, R. Diana-Rivero, S. Delgado-Hernandez, F. Garcia-Tellado, *Org. Lett.* **2018**, 20, 7987–7990.

[28] A. E. Fraley, K. C. Haatveit, Y. Ye, S. P. Kelly, S. A. Newmister, F. Yu, R. M. Williams, J. L. Smith, K. N. Houk, D. H. Sherman, *J. Am. Chem. Soc.* **2020**, 142, 2244–2252.

[29] A. E. Fraley, H. T. Tran, S. P. Kelly, S. A. Newmister, A. Tripathi, H. Kato, S. Tsukamoto, L. Du, S. Li, R. M. Williams, D. H. Sherman, *ChemBioChem* **2020**, 21, 2449–2454.

[30] A. E. Fraley, D. H. Sherman, *FEBS J.* **2020**, 287, 1381–1402.

[31] Y. Ye, L. Du, X. Zhang, S. A. Newmister, M. McCauley, J. V. Alegre-Requena, W. Zhang, S. Mu, A. Minami, A. E. Fraley, M. L. Adrover-Castellano, N. A. Carney, V. V. Shende, F. Qi, H. Oikawa, H. Kato, S. Tsukamoto, R. S. Paton, R. M. Williams, D. H. Sherman, S. Li, *Nat. Catal.* **2020**, 3, 497–506.

[32] S. Li, K. Anand, H. Tran, F. Yu, J. M. Finefield, J. D. Sunderhaus, T. J. McAfoos, S. Tsukamoto, R. M. Williams, D. H. Sherman, *MedChemComm* **2012**, 3, 987–996.

[33] S. Li, J. M. Finefield, J. D. Sunderhaus, T. J. McAfoos, R. M. Williams, D. H. Sherman, *J. Am. Chem. Soc.* **2012**, 134, 788–791.

[34] J. Peng, H. Gao, J. Li, J. Ai, M. Geng, G. Zhang, T. Zhu, Q. Gu, D. Li, *J. Org. Chem.* **2014**, 79, 7895–7904.

[35] Y. Ding, J. R. de Wet, J. Cavalcoli, S. Li, T. J. Greshock, K. A. Miller, J. M. Finefield, J. D. Sunderhaus, T. J. McAfoos, S. Tsukamoto, R. M. Williams, D. H. Sherman, *J. Am. Chem. Soc.* **2010**, 132, 12733–12740.

[36] K. Blin, S. Shaw, H. E. Augustijn, Z. L. Reitz, F. Biermann, M. Alanjary, A. Fetter, B. R. Terlouw, W. W. Metcalf, E. J. N. Helfrich, G. P. van Wezel, M. H. Medema, T. Weber, *Nucleic Acids Res.* **2023**, 51, W46–W50.

[37] K. Gomi, Y. Iimura, S. Hara, *J. Agric. Food Chem.* **1987**, 51, 2549-2555.

[38] W. Zhang, L. Du, Z. Qu, X. Zhang, F. Li, Z. Li, F. Qi, X. Wang, Y. Jiang, P. Men, J. Sun, S. Cao, C. Geng, F. Qi, X. Wan, C. Liu, S. Li, *Proc. Natl. Acad. Sci. U.S.A.* **2019**, 116, 13305–13310.

[39] K. R. Klas, H. Kato, J. C. Frisvad, F. Yu, S. A. Newmister, A. E. Fraley, D. H. Sherman, S. Tsukamoto, Robert M. Williams, *Nat. Prod. Rep.* **2018**, 35, 532–558.

[40] A. Winkler, M. Puhl, H. Weber, T. M. Kutchan, K. Gruber, P. Macheroux, *Phytochemistry* **2009**, 70, 1092–1097.

[41] J. Jumper, R. Evans, A. Pritzel, T. Green, M. Figurnov, O.Ronneberger,K. Tunyasuvunakool, R. Bates, A. Žídek, A. Potapenko, A. Bridgland, C. Meyer, S. A. A. Kohl, A. J. Ballard, A. Cowie, B. Romera-Paredes, S. Nikolov, R. Jain, J. Adler, T. Back, S. Petersen, D. Reiman, E. Clancy, M. Zielinski, M. Steinegger, M. Pacholska, T. Berghammer, S. Bodenstein, D. Silver, O. Vinyals, A. W. Senior, K. Kavukcuoglu, P. Kohli, D. Hassabis, *Nature* **2021**, 596, 583–589.

[42] O. Trott, A. J. Olson, *J. Comput. Chem.* **2010**, 31, 455-461.

[43] B. Daniel, B. Konrad, M. Toplak, M. Lahham, J. Messenlehner, A. Winkler, P. Macheroux, *Arch. Biochem. Biophys.* **2017**, 632, 88–103.

[44] H. Xu, W. Liang, L. Ning, Y. Jiang, W. Yang, C. Wang, F. Qi, L. Ma, L. Du, L. Fourage, Y. J. Zhou, S. Li, *ChemCatChem* **2020**, 12, 80–84.

RESEARCH ARTICLE

Entry for the Table of Contents
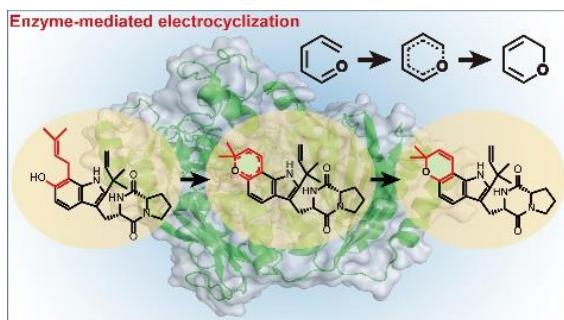
A berberine bridge-like oxidoreductase mediates oxidative electrocyclization to form the 2,2-dimethyl-2*H*-pyran (DMP) ring in fungal indole alkaloids. Heterologous gene expression, *in vitro* enzyme activity reconstitution, and mechanistic studies unveil nature's strategy for pyran formation via enzymatic electrocyclization, expanding biocatalytic pericyclic chemistry.